J Mol Model (2013) 19:2723–2737
DOI 10.1007/s00894-012-1540-y

ORIGINAL PAPER

Bis(heptalene) "submarine" metal dimer sandwich compounds $(C_{12}H_{10})_2M_2$ (M = Ti, V, Cr, Mn, Fe, Co, Ni)

Huidong Li · Hao Feng · Weiguo Sun · Qunchao Fan · Yaoming Xie · R. Bruce King · Henry F. Schaefer III

Received: 3 May 2012 / Accepted: 16 July 2012 / Published online: 14 August 2012

Abstract The bis(heptalene)dimetal complexes $(C_{12}H_{10})_2M_2$ of the first row transition metals from Ti to Ni are predicted by density functional theory to exhibit "submarine" sandwich structures with a pair of metal atoms sandwiched between the two heptalene rings. For the early transition metal derivatives $(C_{12}H_{10})_2M_2$ (M = V, Cr) there are two types of such structures. In one structural type the metals are sandwiched between two heptahapto heptalene rings with metal-metal distances (3.5–3.8 Å) too long for direct metal-metal bonding. The other type of $(C_{12}H_{10})_2M_2$ (M = V, Cr, Mn) structure has a pair of bonded metal atoms sandwiched between a fully bonded heptalene ligand and a heptalene ligand bonded to the metals only through an eight-carbon heptafulvene subunit, leaving an uncomplexed *cis*-1,3-diene unit. The formal metal-metal bond orders in these latter structures are 3, 2, and 1 for M = V, Cr, and Mn with predicted bond lengths of 2.5, 2.7, and 2.8 Å, respectively. For $(C_{12}H_{10})_2Fe_2$ a singlet structure with each iron atom sandwiched between a hexahapto and a tetrahapto heptalene ring is energetically preferred over an alternate structure with ferrocene-like iron atoms sandwiched between two pentahapto heptalene rings. Partial bonding of each heptalene ring to the metal atoms occurs in the late transition metal derivatives $(C_{12}H_{10})_2M_2$ (M = Co, Ni). This leads to an unsymmetrical structure for the cobalt derivative and a structure for the nickel derivative with each nickel atom sandwiched between a trihapto ligand and a tetrahapto ligand.

Keywords Density functional theory · Heptalene · Sandwich compounds · Transition metal

Electronic supplementary material The online version of this article (doi:10.1007/s00894-012-1540-y) contains supplementary material, which is available to authorized users.

H. Li · H. Feng (✉) · W. Sun · Q. Fan
School of Physics and Chemistry, Research Center for Advanced Computation, Xihua University,
Chengdu 610039, China
e-mail: Fenghao@mail.xhu.edu.cn

H. Li · H. Feng · W. Sun
Institute of Atomic and Molecular Physics, Sichuan University,
Chengdu, Sichuan 610065, China

Y. Xie · R. B. King (✉) · H. F. Schaefer III
Department of Chemistry and Center for Computational Chemistry, University of Georgia,
Athens, GA 30602, USA
e-mail: rbking@chem.uga.edu

Introduction

A key development in transition metal organometallic chemistry was the 1951 discovery of ferrocene [1, 2], $(\eta^5\text{-}C_5H_5)_2Fe$, having a then unprecedented structure with an iron atom sandwiched between two planar parallel cyclopentadienyl rings. Shortly thereafter, many other transition metals, particularly those in the first row from vanadium to nickel, were also found to form similar sandwich compounds $(\eta^5\text{-}C_5H_5)_2M$, isostructural with ferrocene. A subsequent milestone was the discovery of the related sandwich compound dibenzenechromium [3], $(\eta^6\text{-}C_6H_6)_2Cr$ in 1955 (Fig. 1). At that time the idea of sandwiching a metal atom between two stable benzene molecules to give a thermally stable sandwich compound was truly revolutionary.

The concept of sandwich compounds having a metal located between two planar parallel carbocyclic rings can be extended to "submarine sandwiches" in which a pair of metal atoms is sandwiched between two planar bicyclic hydrocarbons. The obvious idea of sandwiching a pair of metal atoms between two planar naphthalene rings has not yet been achieved although two naphthalene ligands can sandwich a single chromium atom in $(\eta^6\text{-}C_{10}H_8)_2Cr$ with a local chromium environment similar to that in dibenzenechromium [4]

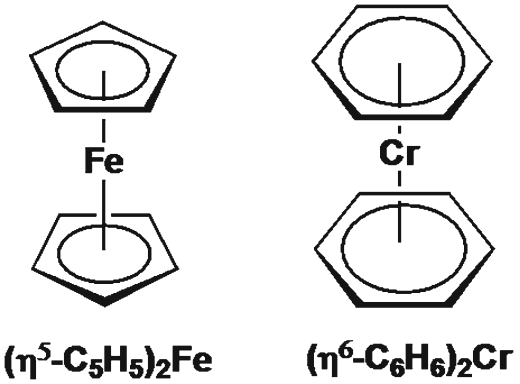

Fig. 1 Structures of ferrocene and dibenzenechromium

(Fig. 2). This leaves an uncomplexed *cis* 1,3-diene system in each naphthalene ring.

The bicyclic non-benzenoid hydrocarbon pentalene (Fig. 3) has proven to be a more successful ligand for "submarine sandwich" compounds (Fig. 4). The first reports of possible such compounds date back to the syntheses in 1972 of the dicobalt and dinickel derivatives $(C_8H_6)_2M_2$ (M = Co [5], Ni [6]) by Katz and co-workers. However, the structures of these possible submarine sandwich compounds have never been confirmed by X-ray crystallography. Relatively recently (2008) O'Hare and co-workers [7] have shown that complete substitution of the six hydrogen atoms in pentalene with methyl groups leads to the bis (hexamethylpentalene)metal derivatives $(C_8Me_6)_2M_2$ (M = V, Cr, Mn, Co, Ni), which have been shown by X-ray crystallography to have submarine sandwich structures. In addition Cloke and co-workers [8–10] have synthesized the related silylated bis(pentalene)metal derivatives $Mo_2[C_8H_4(SiPr_3)_2]_2$, $Cr_2[C_8H_4(SiPr_3)_2]_2$, and $Mn_2[C_8H_4(SiPr_3)_2]_2$.

The bicyclic non-benzenoid hydrocarbon heptalene (Fig. 3) was first synthesized by Dauben and Bertelli in 1961 [11]. The first metal carbonyl derivative of heptalene, namely $(\eta^6\text{-}C_{12}H_{10})Cr(CO)_3$, was synthesized 13 years later by Vogel et al. [12, 13]. Subsequently mononuclear and

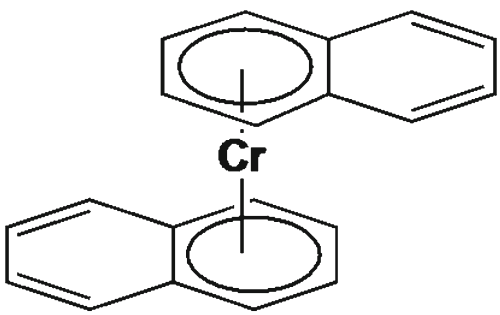

Fig. 2 The structure of dinaphthalenechromium showing the two uncomplexed C = C double bonds in each naphthalene ring

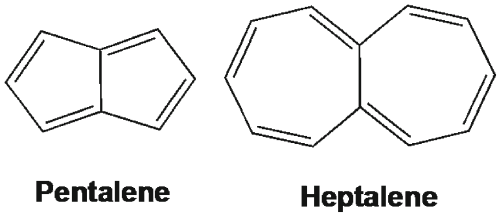

Fig. 3 Structures of pentalene and heptalene

binuclear iron carbonyl derivatives of heptalene were synthesized with η^4 coordination of $Fe(CO)_3$ groups to two of the double bonds in the heptalene system [14–16]. Similar iron carbonyl complexes of 1,6-dimethylheptalene have also been synthesized [16]. However, carbonyl-free sandwich compounds of heptalene or its derivatives have not yet been synthesized.

This paper reports a systematic density functional theory investigation of the bis(heptalene)dimetal complexes $(C_{12}H_{10})_2M_2$ (M = Ti, V, Cr, Mn, Fe, Co, Ni). An interesting feature of many of these complexes is a metal-metal distance too long to imply any direct metal-metal bonding. The early transition metal $(C_{12}H_{10})_2M_2$ complexes have submarine sandwich structures in which all seven carbon atoms of each heptalene ring participate in the metal-ring bonding, leading to a bis(heptahaptoheptalene) metal environment for each metal atom. However, alternative structures are also found for the early transition metal $(C_{12}H_{10})_2M_2$ derivatives in which only one of the heptalene ligands is fully bonded to the pair of metal atoms. In these latter structures the other heptalene ligand is highly non-planar and uses only eight carbons of a heptafulvene subunit for bonding to the pair of metal atoms, leaving an uncomplexed 1,3-diene unit. The heptalene ligands in the $(C_{12}H_{10})_2M_2$ complexes of the later transition metals Fe, Co, and Ni, which require fewer ligand electrons to attain the favored 18-electron configuration, have carbon atoms outside reasonable bonding distances of either metal atom.

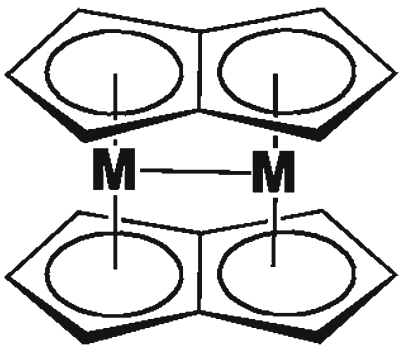

Fig. 4 Schematic representation of the bis(pentalene)dimetal submarine sandwich structures, omitting for clarity the external pentalene substituents (methyl in the O'Hare hexamethylpentalene derivatives [7]) and not assigning formal orders of the metal-metal bond

Theoretical methods

Double-ζ plus polarization (DZP) basis sets were used in this research. For carbon one set of pure spherical harmonic d functions with orbital exponent $\alpha_d(C)=0.75$ is added to the standard Huzinaga-Dunning contracted DZ sets. This basis set is designated (9s5p1d/4s2p1d) [17, 18]. For H, a set of p polarization functions $\alpha_p(H)=0.75$ is added to the Huzinaga-Dunning DZ sets. For the first row transition metals, in our loosely contracted DZP basis sets, the Wachters' primitive sets are used [19], but augmented by two sets of p functions and one set of d functions, contracted following Hood et al., and designated (14s11p6d/10s8p3d) [20].

Electron correlation effects have been included to some degree using density functional theory (DFT) methods, which have evolved as a practical and effective computational tool, especially for organometallic compounds [21–27]. The reliability of such density functional theory (DFT) methods is governed by the quality of the approximate exchange-correlation (XC) energy functional. Three differently constructed DFT functionals, namely the B3LYP* method, the BP86 method and the M06-L method, were used in the present study. The original B3LYP method is a hybrid HF/DFT method, combining the three-parameter Becke functional (B3) with the Lee-Yang-Parr (LYP) generalized gradient correlation functional [28, 29]. This method includes exact exchange and is calibrated by fitting three parameters to a set of experimental results. However, decreasing the amount of the Hartree-Fock exchange from the 20 % incorporated in the original hybrid density functional B3LYP to the 15 % used in the newer B3LYP* has been shown to describe more accurately complexes of first row transition metals. Therefore the newer B3LYP* method rather than the original B3LYP was used [30–32]. The BP86 method combines Becke's 1988 exchange functional (B) with Perdew's 1986 gradient-corrected correlation functional method (P86) [33, 34]. This method does not include exact exchange and is mainly deduced by forcing the functional to satisfy certain exact constraints based on first principles. The third functional used in this work is a hybrid *meta*-GGA DFT method, M06-L, developed by Truhlar's group [35]. This functional reflects considerable progress by Truhlar's group toward the development of improved exchange-correlation functional that are essential for expanding the applicability of Kohn-Sham DFT. The M06-L functional was constructed using three strategies, namely constraint satisfaction, modeling the exchange-correlation hole, and empirical testing. The studies in Truhlar's group suggest that M06-L is one of the best functionals for the study of organometallic and inorganic thermochemistry, and may be the best functional for transition metal energetics. When these three conceptually different DFT methods agree, confident predictions can be made.

The geometries of all structures were first fully optimized using the DZP BP86 method with the default fine grid (75, 302) for evaluating integrals numerically in Gaussian09 [36]. Subsequently, all of the structures were reoptimized with the DZP B3LYP* and DZP M06-L methods using the ultrafine grid (99, 590) in order to enhance the reliability of the results. Harmonic vibrational frequencies were determined at the same levels by evaluating analytically the second derivatives of the energy with respect to the nuclear coordinates. The corresponding infrared intensities were evaluated analytically as well. The tight designation is the default for the energy convergence. For structures with small imaginary vibrational frequencies, the much finer integration grid (120, 974) was used for further evaluation.

In the search for minima, low-magnitude imaginary vibrational frequencies may be suspect, because the numerical integration procedures used in existing DFT methods have significant limitations [37]. All of the final optimized structures reported in this paper have only real vibrational frequencies unless otherwise indicated.

The geometries of $(C_{12}H_{10})_2M_2$ (M = Ti to Ni) were optimized for the lowest energy singlet and triplet electronic states. The optimized geometries of the energetically low-lying $(C_{12}H_{10})_2M_2$ structures are shown in Figs. 5, 6, 7, 8, 9, 10 and 11. In all of the figures the listed distances (in Ångstroms) were obtained using the M06-L method. Each structure is designated as **M-nX**, where **M** is the symbol of the central metal atom, **n** orders the structures according to their relative energies predicted by the BP86 method, and **X** designates the spin states, using **S** and **T** for the singlets and triplets, respectively.

Figures S1–S7 are available in supplementary material.

Results

$(C_{12}H_{10})_2Ti_2$

Four $(C_{12}H_{10})_2Ti_2$ structures, namely two singlet structures **Ti-2S** and **Ti-3S** and two triplet structures **Ti-1T** and **Ti-4T**, have been optimized (Figs. 5 and S1, Table 1). The global minimum is a triplet (η^5,η^7-$C_{12}H_{10})_2Ti_2$ structure **Ti-1T** with C_{2h} (B3LYP*) or C_2 (BP86 and M06-L) symmetry. Each Ti atom in **Ti-1T** is sandwiched between a pentahapto ring and a heptahapto ring, as indicated by the Ti-C distances. The predicted Ti-Ti distance of 3.371 Å (B3LYP*), 3.478 Å (BP86), or 3.310 Å (M06-L) suggests a formal single bond, so that each titanium atom in **Ti-1T** has a

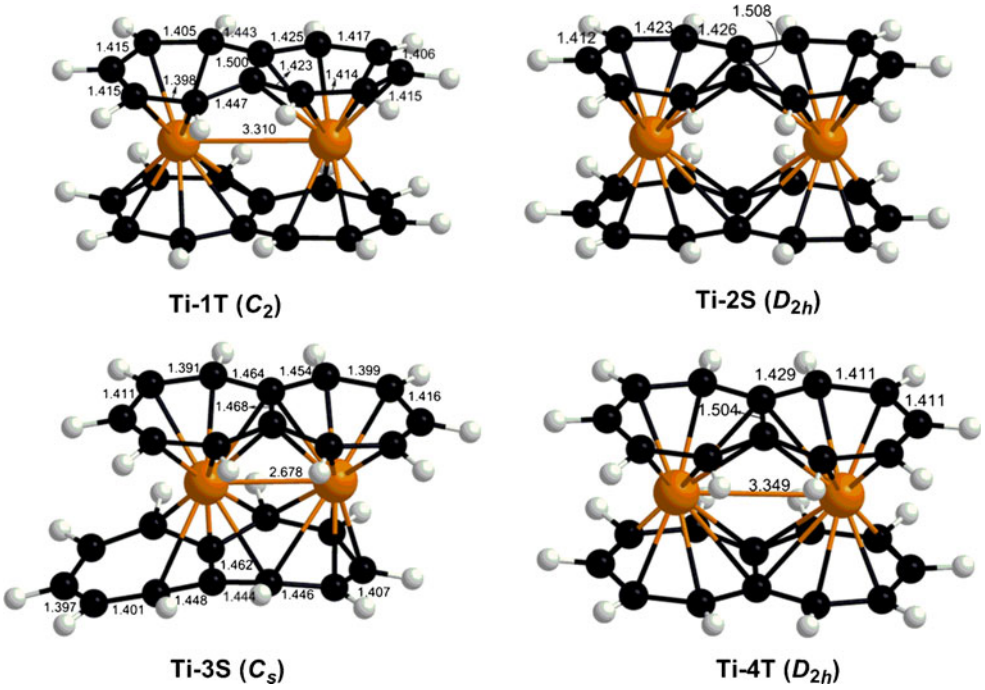

Fig. 5 The four optimized $(C_{12}H_{10})_2Ti_2$ structures. The distances listed in Figs. 5, 6, 7, 8, 9, 10 and 11 were obtained by the M06-L method

17-electron configuration, which is consistent with a binuclear triplet.

The singlet **Ti-2S** with a bis(heptahapto) structure (η^7,η^7-$C_{12}H_{10})_2Ti_2$ lies 4.7 kcal mol^{-1} (B3LYP*) above **Ti-1T**, is nearly degenerate with **Ti-1T** (BP86), or lies 3.3 kcal mol^{-1} (M06-L) above **Ti-1T** (Figs. 5 and S1, Table 1). A small imaginary vibrational frequency of 26*i* cm^{-1} was found by the M06-L method, which cannot be removed even by using the finer grid. The predicted Ti···Ti distance of 3.741 Å (B3LYP*), 3.754 Å (BP86), or 3.670 Å (M06-L) indicates the lack of a titanium-titanium bond. Thus each titanium atom in **Ti-2S** has a 16-electron configuration similar to the titanium atoms in the mononuclear derivatives (η^5-C_5H_5)(η^7-C_7H_7)Ti [38] and (η^6-$CH_3C_6H_5)_2$Ti [39], assuming that the 12 π-electrons of each heptalene ring are divided equally between the two titanium atoms.

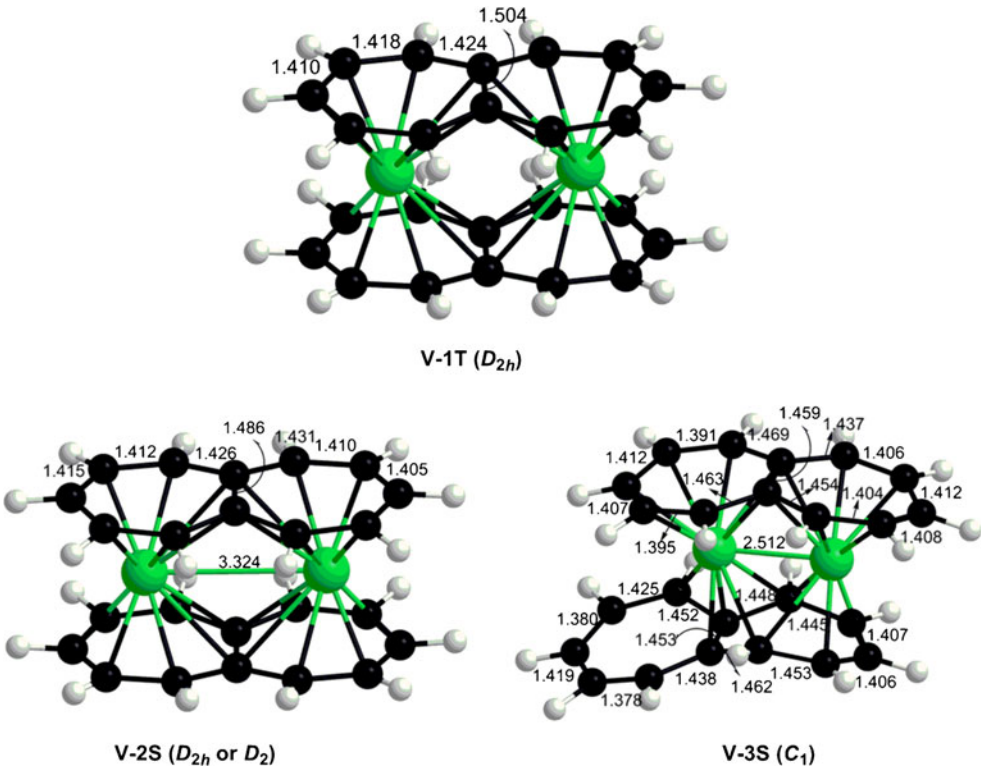

Fig. 6 The three optimized $(C_{12}H_{10})_2V_2$ structures

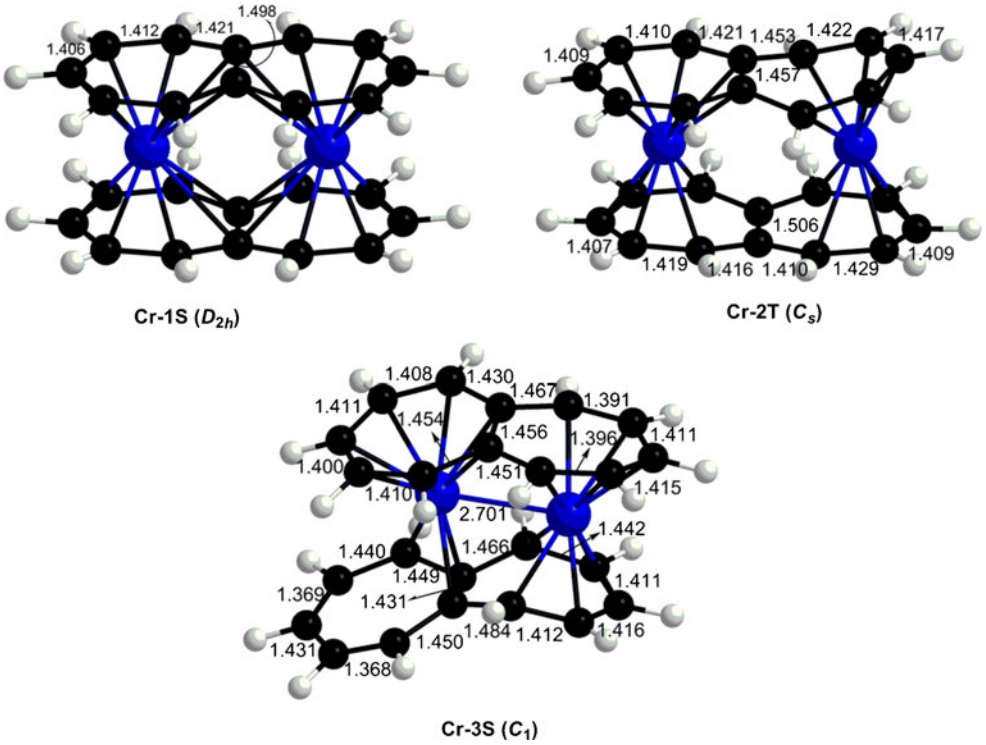

Fig. 7 The three optimized $(C_{12}H_{10})_2Cr_2$ structures

Another singlet $(C_{12}H_{10})_2Ti_2$ structure **Ti-3S** with C_s symmetry lies 7.3 kcal mol^{-1} above the global minimum **Ti-1T** by the B3LYP* method, but is essentially degenerate with **Ti-1T** by the BP86 and M06-L methods (Figs. 5 and S1, Table 1). In **Ti-3S** one of the heptalene ligands uses all 12 carbon atoms to bond to the Ti_2 unit as a heptahapto ligand to each titanium atom. However, the other heptalene ligand is only partially bonded to the central Ti_2 unit with seven carbon atoms within ~2.6 Å of at least one Ti atom and two additional carbon atoms within ~2.7 Å of one of the Ti atoms. The remaining three carbon atoms of this non-planar heptalene unit are more than ~3.5 Å from either Ti atom, and thus are not directly involved in ligand-metal bonding. The Ti≡Ti distance in **Ti-3S** of 2.738 Å (B3LYP*), 2.695 Å (BP86), or 2.678 Å (M06-L) can correspond to a formal triple bond. There are no experimental examples of such Ti≡Ti triple bonds. However, the yet unknown molecule $(\eta^5\text{-}C_5H_5)_2Ti_2(CO)_6$ is predicted [40] to have a Ti≡Ti triple bond distance of 2.80 Å. A formal Ti≡Ti triple bond gives one titanium atom in **Ti-3S** the favored 18-electron configuration but the other titanium atom only a 16-electron configuration. This assumes that the fully bonded heptalene ring donates all 12 π-electrons to the Ti_2 system but the other heptalene ring donates only eight π-electrons to the Ti_2 system for a total of 20 electrons from the two heptalene ligands.

The remaining $(C_{12}H_{10})_2Ti_2$ structure is the D_{2h} triplet **Ti-4T**, predicted to lie 8.1 kcal mol^{-1} (B3LYP*), 0.5 kcal mol^{-1} (BP86), or 0.9 kcal mol^{-1} (M06-L) above the global minimum **Ti-1T** (Figs. 5, S1, and Table 1). Structure **Ti-4T** is found to have two imaginary vibrational frequencies of 418i cm^{-1} and 60i cm^{-1} (B3LYP*), 81i cm^{-1} (BP86), or 61i cm^{-1} and 30i cm^{-1} (M06-L), which are not removed by using the finer integration grid. Following the normal mode corresponding to these imaginary vibrational frequencies leads to the global minimum **Ti-1T**. The Ti-C distances indicate **Ti-4T** to be a bis(heptahapto) structure $(\eta^7,\eta^7\text{-}C_{12}H_{10})_2Ti_2$ very much like **Ti-2S**. The Ti-Ti

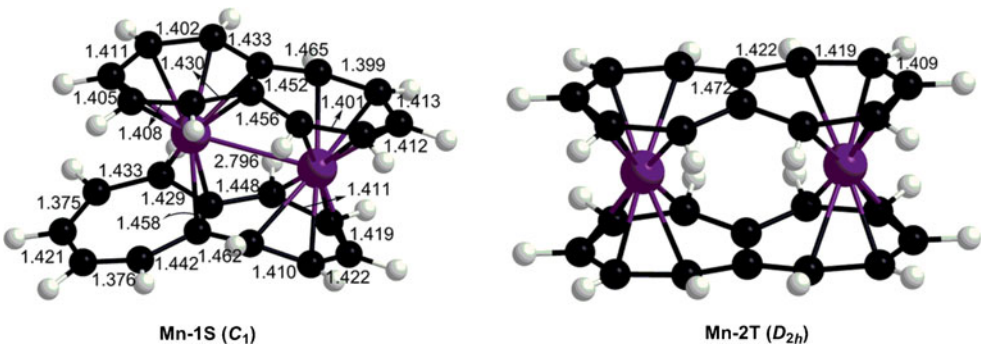

Fig. 8 The two optimized $(C_{12}H_{10})_2Mn_2$ structures

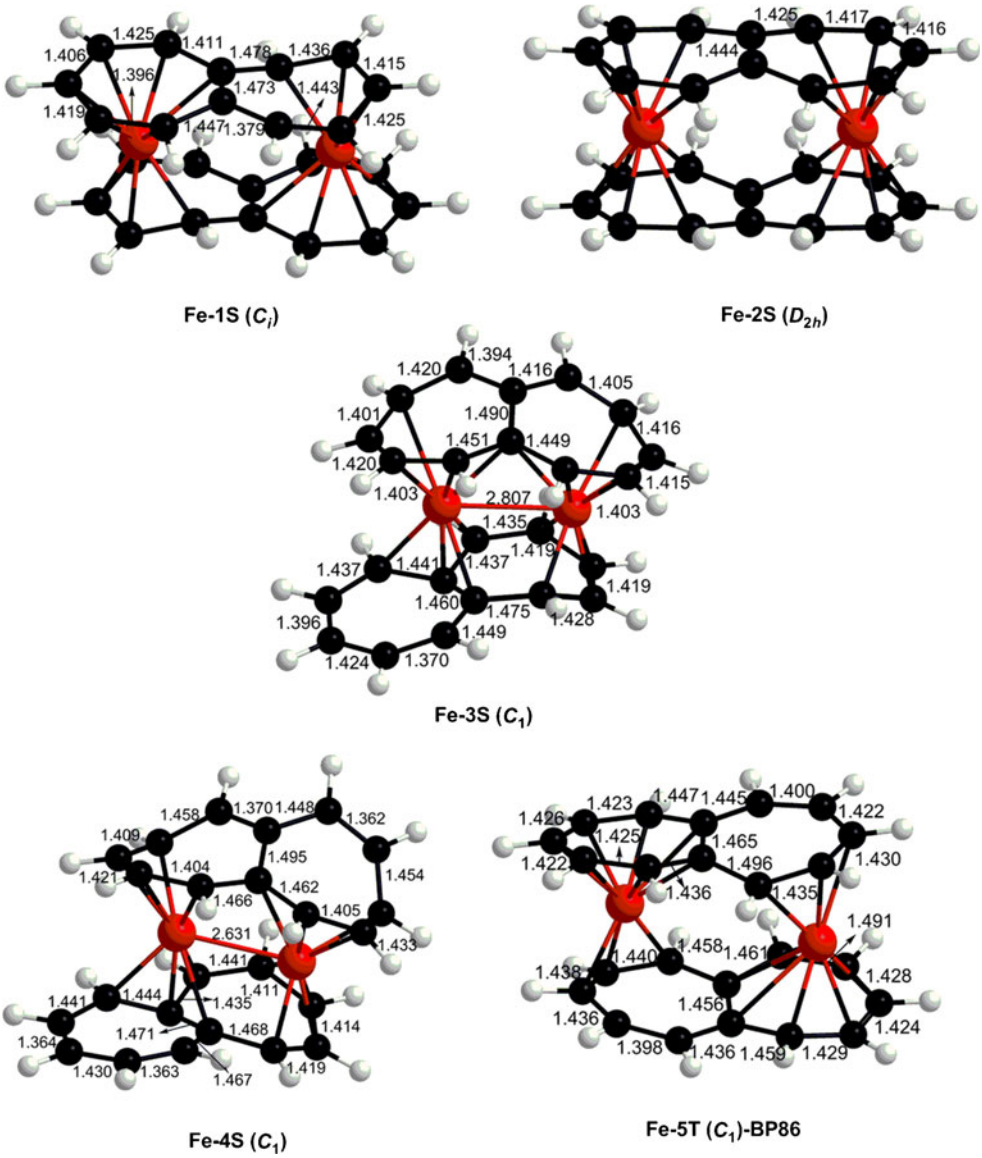

Fig. 9 Optimized $(C_{12}H_{10})_2Fe_2$ structures

distance of 3.435 Å (B3LYP*), 3.461 Å (BP86), or 3.349 Å (M06-L) in **Ti-4T** can be interpreted as a formal single bond thereby giving each Ti atom the 17-electron configuration, consistent with a binuclear triplet.

The fact that three different optimized stable structures (**Ti-1T**, **Ti-2S**, and **Ti-3S**) by the BP86 and M06-L methods have essentially identical energies appears to be a very strange coincidence. In order to confirm the correctness of this apparently unlikely observation, additional BP86 optimizations were performed on $(C_{12}H_{10})_2Ti_2$ starting from the B3LYP* geometries. The two singlet structures **Ti-2S** and **Ti-3S** and their energies were reproduced as obtained from the initial optimizations. The global minimum **Ti-1T** was eventually obtained after optimization of the orbital stability. We therefore suspect that **Ti-1T** is the strongly preferred structure for $(C_{12}H_{10})_2Ti_2$.

$(C_{12}H_{10})_2V_2$

Three structures (**V-1T**, **V-2S**, and **V-3S)** were found for the binuclear vanadium compound $(C_{12}H_{10})_2V_2$ (Figs. 6 and S2, Table 2)**.** The global minimum structure is the D_{2h} triplet **V-1T.** The V-C distances in **V-1T** indicate each heptalene ring to function as a heptahapto ligand toward a single vanadium atom. The V···V distance of 3.606 Å (B3LYP*), 3.616 Å (BP86) or 3.519 Å (M06-L) in **V-1T** suggests no direct bond between the two vanadium atoms, thereby giving each vanadium atom the 17-electron configuration for a binuclear triplet. This global minimum structure **V-1T** predicted by the M06-L method was found to have a small imaginary frequency of 22*i* cm^{-1}, which cannot be removed by using the finer grid. The local environment for the vanadium atoms in **V-1T** is similar to that in the known

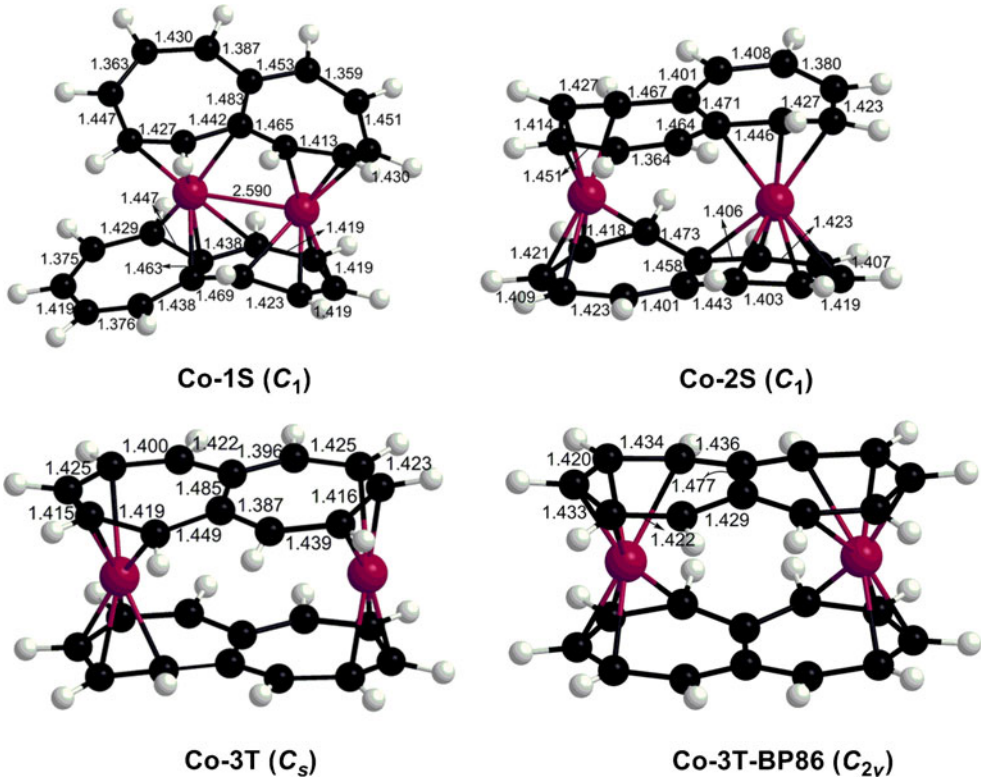

Fig. 10 Optimized $(C_{12}H_{10})_2Co_2$ structures

stable compounds $(\eta^5\text{-}C_5H_5)(\eta^7\text{-}C_7H_7)V$ [41, 42] and $(\eta^6\text{-}C_6H_6)_2V$ [43].

The two singlet $(C_{12}H_{10})_2V_2$ structures lie at significantly higher energies than the triplet global minimum **V-1T** (Figs. 6 and S2, Table 2). The $(C_{12}H_{10})_2V_2$ structure **V-2S**, lying 32.8 kcal mol^{-1} (B3LYP*), 14.0 kcal mol^{-1} (BP86), or 17.1 kcal mol^{-1} (M06-L) in energy above the global minimum **V-1T**, has each vanadium atom sandwiched between

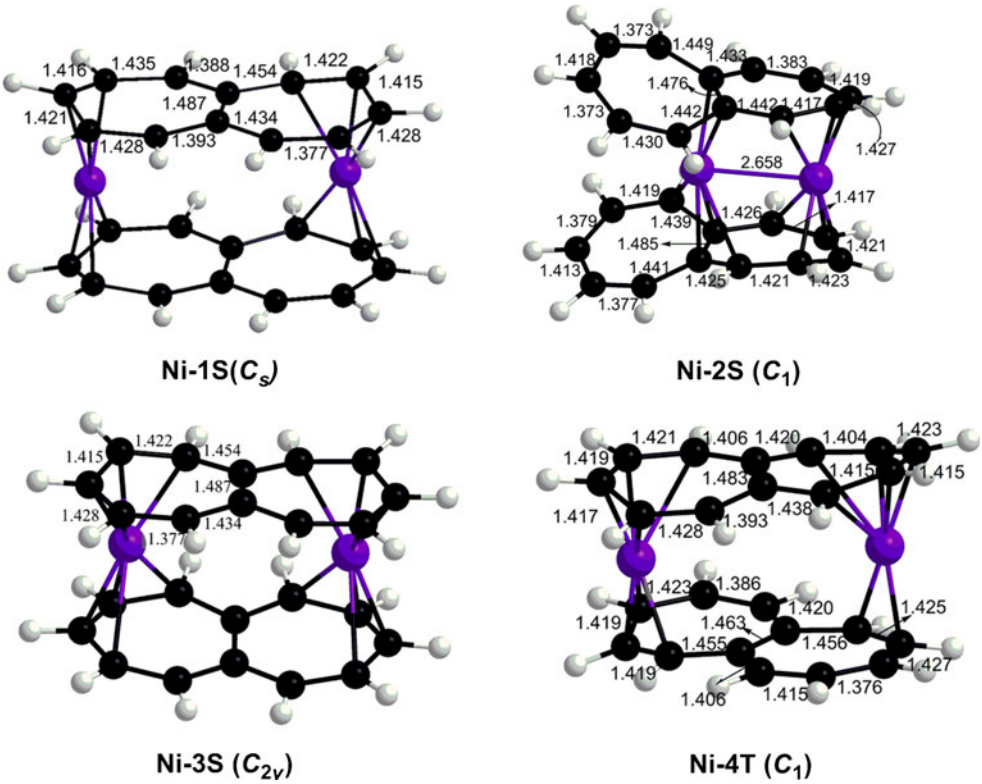

Fig. 11 The optimized $(C_{12}H_{10})_2Ni_2$ structures

Table 1 Total energies (E in hartree), relative energies (ΔE in kcal mol^{-1}), HOMO-LUMO gaps (eV), Ti-Ti distances (Å), numbers of imaginary vibrational frequencies (Nimg), and spin expectation values $\langle S^2 \rangle$ for the $(C_{12}H_{10})_2Ti_2$ structures

	B3LYP*	BP86	M06-L	B3LYP*	BP86	M06-L
	Ti-1T (C_2 or C_{2h})			Ti-2S (D_{2h})		
-HOMO(α)	0.14209	0.12410	0.11966	0.14357	0.13442	0.12862
-LUMO(α)	0.08591	0.11243	0.10484	0.08429	0.11690	0.11037
gap/eV	1.53	0.32	0.40	1.61	0.48	0.50
Ti-Ti	3.371	3.478	3.310	3.741	3.754	3.670
–E	2624.75334	2625.90776	2625.53109	2624.74578	2625.90775	2625.52580
ΔE	0.0	0.0	0.0	4.7	0.0	3.3
Nimg	none	none	none	none	none	26i
$\langle S^2 \rangle$	2.08	2.02	2.05	0.00	0.00	0.00
	Ti-3S (C_s)			Ti-4T (D_{2h})		
-HOMO(α)	0.14235	0.13158	0.12924	0.13758	0.12951	0.12553
-LUMO(α)	0.08540	0.10698	0.10205	0.10577	0.11506	0.11186
gap/eV	1.55	0.67	0.74	0.87	0.39	0.37
Ti-Ti	2.738	2.695	2.678	3.435	3.461	3.349
–E	2624.74169	2625.90783	2625.53131	2624.74041	2625.90698	2625.52970
ΔE	7.3	0.0	–0.1	8.1	0.5	0.9
Nimg	none	none	none	2(418i,60i)	1 (81i)	2(61i,30i)
$\langle S^2 \rangle$	0.00	0.00	0.00	2.04	2.02	2.03

two heptahapto heptalene rings. The predicted V-V distance of 3.508 Å (B3LYP*), 3.539 Å (BP86), or 3.324 Å (M06-L) in **V-2S** can correspond to a formal single bond, leading to the favored 18-electron configuration for each vanadium atom in **V-2S**. For comparison, the predicted length for a singly carbonyl-bridged V-V single bond in $(\eta^5\text{-}C_5H_5)_2V_2(CO)_7$ is ~3.35 Å [44]. The longer V-V single bond in **V-2S** may be a consequence of the geometrical constraints of the two heptalene rings forming the sandwich structure.

The other singlet $(C_{12}H_{10})_2V_2$ structure **V-3S** is a relatively high energy structure, lying 31.5 kcal mol^{-1} (B3LYP*) or 23.9 kcal mol^{-1} (BP86 and M06-L) in energy above the global minimum structure **V-1T** (Figs. 6 and S2, Table 2). One heptalene ligand in **V-3S** uses all 12 carbon atoms to bond to the V_2 unit whereas the other heptalene ligand uses only eight carbon atoms of a heptafulvene subunit for the ligand-metal bonding (Figs. 6 and S2, Table 2). This leaves an uncomplexed 1,3-diene unit in the latter heptalene ligand, which is highly non-planar and has relatively short uncomplexed C=C distances of 1.38 Å (B3LYP* and M06-L) or 1.39 Å (BP86). The V≡V distance of 2.529 Å (B3LYP*), 2.546 Å (BP86), or 2.512 Å (M06-L) in **V-3S** may be interpreted as a formal triple bond, thereby giving each vanadium atom the favored 18-electron configuration. For comparison, the experimental value of the V≡V triple bond distance in $(\eta^5\text{-}C_5H_5)_2V_2(CO)_5$ is 2.459 Å, as determined by X-ray diffraction [45, 46].

Table 2 Total energies (E in hartree), relative energies (ΔE in kcal mol^{-1}), HOMO-LUMO gaps (eV), V-V distances (Å), numbers of imaginary vibrational frequencies (Nimg), and spin expectation values $\langle S^2 \rangle$ for the $(C_{12}H_{10})_2V_2$ structures

	V-1T (D_{2h})			V-2S (D_{2h} or D_2)			V-3S (C_1)		
	B3LYP*	BP86	M06-L	B3LYP*	BP86	M06-L	B3LYP*	BP86	M06-L
HOMO(α)	0.13935	0.13203	0.12649	0.13808	0.12988	0.12490	0.13054	0.11843	0.11393
LUMO(α)	0.06110	0.08282	0.07585	0.10999	0.11908	0.10922	0.07626	0.09993	0.09119
gap/eV	2.13	1.34	1.38	0.76	0.29	0.43	1.48	0.50	0.62
V-V	3.606	3.616	3.519	3.508	3.539	3.324	2.529	2.546	2.512
–E	2813.79539	2815.01769	2814.57463	2813.74313	2814.99544	2814.54741	2813.74523	2814.97955	2814.53657
ΔE	0.0	0.0	0.0	32.8	14.0	17.1	31.5	23.9	23.9
Nimg	none	none	1(22i)	none	none	none	none	none	none
$\langle S^2 \rangle$	2.07	2.05	2.11	0.00	0.00	0.00	0.00	0.00	0.00

$(C_{12}H_{10})_2Cr_2$

Three structures, namely the D_{2h} singlet **Cr-1S**, the C_s triplet **Cr-2T**, and the C_1 singlet **Cr-3S** are predicted for the binuclear chromium sandwich $(C_{12}H_{10})_2Cr_2$ (Figs. 7 and S3, Table 3). The global minimum structure predicted by the BP86 method is the singlet structure **Cr-1S**, with each chromium atom bonded to two heptahapto ligands, as indicated by the Cr-C distances. The long Cr···Cr distance of 3.535 Å (B3LYP*), 3.549 Å (BP86), or 3.443 Å (M06-L) suggests the absence of direct bonding between the chromium atoms. Each chromium atom in **Cr-1S** acquires the favored 18-electron configuration if the 12 π-electrons from each heptalene ring are split equally between the chromium atoms. In **Cr-1S** a small imaginary frequency of 9i cm^{-1} is predicted by the M06-L method, however, it can be removed using the finer grid.

The second $(C_{12}H_{10})_2Cr_2$ structure is the triplet structure **Cr-2T** lying 3.7 kcal mol^{-1} (B3LYP* and M06-L) below or 0.5 kcal mol^{-1} above (BP86) the global minimum structure **Cr-1S** (Figs. 7 and S3, Table 3). Structure **Cr-2T** has one chromium atom bonded to ten carbon atoms in two pentahapto heptalene rings with a local environment similar to the known [47] $(\eta^5\text{-}C_5H_5)_2Cr$, which is a stable triplet molecule. The other chromium atom is bonded to 12 carbon atoms in one pentahapto and one heptahapto heptalene ring and thus has a local environment similar to that of the known [48, 49] $(\eta^5\text{-}C_5H_5)Cr(\eta^7\text{-}C_7H_7)$. Significant spin contamination ($\langle S^2\rangle$ = 2.34 or 2.41) is predicted for **Cr-2T** by the B3LYP* and BP86 methods. The calculated Cr···Cr distance of 3.916 Å (B3LYP*), 3.885 Å (BP86), or 3.854 Å (M06-L) in **Cr-2T** is too long for a conventional chromium-chromium bond. In **Cr-2T** the chromium atom bonded to a total of 12 heptalene carbon atoms has the favored 18-electron configuration whereas the other chromium atom bonded to only ten heptalene carbon atoms has only a 16-electron configuration, similar to that in $(\eta^5\text{-}C_5H_5)_2Cr$. The latter chromium atom accounts for the triplet spin state of **Cr-2T**.

A second singlet $(C_{12}H_{10})_2Cr_2$ structure **Cr-3S**, lying 17.0 kcal mol^{-1} (B3LYP*), 10.1 kcal mol^{-1} (BP86), or 10.3 kcal mol^{-1} (M06-L) above **Cr-1S**, is similar to the $(C_{12}H_{10})_2V_2$ structure **V-3S**. Thus one heptalene ligand in **Cr-3S** uses all 12 of its carbon atoms to bond to the Cr_2 unit whereas the other heptalene ligand uses only eight carbon atoms of a heptafulvene subunit for the ligand-metal bonding (Figs. 7, S3, and Table 3). This leaves an uncomplexed 1,3-diene unit in the latter heptalene ligand, which is highly non-planar. The predicted Cr=Cr distance of 2.752 Å (B3LYP*), 2.777 Å (BP86), or 2.701 Å (M06-L) in **Cr-3S** is consistent with a formal double bond, thereby giving each chromium atom the favored 18-electron configuration.

$(C_{12}H_{10})_2Mn_2$

Two $(C_{12}H_{10})_2Mn_2$ structures (**Mn-1S**, **Mn-2T)** were optimized (Figs. 8 and S4, Table 4). The global minimum structure is the singlet C_1 structure **Mn-1S**. This structure is closely related to the $(C_{12}H_{10})_2M_2$ structures **V-3S** and **Cr-3S**. Thus in **Mn-1S** one heptalene ligand uses all 12 of its carbon atoms to bond to the Mn_2 unit whereas the other heptalene ligand uses only eight carbon atoms of a heptafulvene subunit for ligand-metal bonding (Figs. 8 and S4, Table 4). This leaves an uncomplexed 1,3-diene unit in the latter highly non-planar heptalene ligand having uncomplexed C=C double bonds of lengths 1.37 Å (B3LYP* and M06-L) or 1.39 Å (BP86). The predicted Mn–Mn distance of 2.864 Å (B3LYP*), 2.859 Å (BP86), or 2.796 Å (M06-L) in **Mn-1S** is ~0.1 Å longer than the predicted Cr=Cr double bond distance in **Cr-3S** and is close to the experimental Mn–Mn single bond length in $Mn_2(CO)_{10}$ of 2.895 Å, determined by X-ray crystallography [50]. Thus the Mn-Mn bond in **Mn-1S** can be interpreted as a formal single bond, thereby giving each manganese atom the favored 18-electron configuration.

Table 3 Total energies (E in hartree), relative energies (ΔE in kcal mol^{-1}), HOMO-LUMO gaps (eV), Cr-Cr distances (Å), and spin expectation values $\langle S^2\rangle$ for the $(C_{12}H_{10})_2Cr_2$ structures

	Cr-1S (D_{2h})			Cr-2T (C_s)			Cr-3S (C_1)		
	B3LYP*	BP86	M06-L	B3LYP*	BP86	M06-L	B3LYP*	BP86	M06-L
HOMO(α)	0.16041	0.11819	0.12050	0.14790	0.11991	0.12055	0.14858	0.12051	0.11869
LUMO(α)	0.13690	0.09125	0.07973	0.07558	0.09488	0.08910	0.08332	0.11364	0.10093
gap/eV	0.64	0.73	1.11	1.97	0.66	0.86	1.78	0.17	0.48
Cr-Cr	3.535	3.549	3.443	3.916	3.885	3.854	2.752	2.777	2.701
–E	3014.65439	3015.93918	3015.43273	3014.66024	3015.93834	3.15.43873	3014.62727	3015.92309	3015.41629
Nimg	none	none	1(9i)	none	none	none	none	none	none
ΔE	0.0	0.0	0.0	−3.7	0.5	−3.7	17.0	10.1	10.3
$\langle S^2\rangle$	0.00	0.00	0.00	2.34	2.14	2.41	0.00	0.00	0.00

Table 4 Total energies (E in hartree), relative energies (ΔE in kcal mol^{-1}), HOMO-LUMO gaps (eV), Mn-Mn distances (Å), numbers of imaginary vibrational frequencies (Nimg), and spin expectation values $\langle S^2 \rangle$ for the $(C_{12}H_{10})_2Mn_2$ structures

	Mn-1S (C_1)			Mn-2T (D_{2h})		
	B3LYP*	BP86	M06-L	B3LYP*	BP86	M06-L
-HOMO(α)	0.15102	0.13363	0.13124	0.14937	0.12037	0.12015
-LUMO(α)	0.06505	0.08842	0.07741	0.07708	0.08976	0.08724
gap/eV	2.34	1.23	1.46	1.87	0.83	0.90
Mn-Mn	2.864	2.859	2.796	3.972	4.001	3.907
–E	3327.64959	3329.01001	3328.44063	3327.66309	3229.00332	3328.43776
ΔE	0.0	0.0	0.0	−8.5	4.2	1.8
Nimg	none	none	none	none	none	none
$\langle S^2 \rangle$	0.00	0.00	0.00	2.48	2.12	2.34

The second structure predicted for $(C_{12}H_{10})_2Mn_2$ is the D_{2h} triplet structure **Mn-2T**, lying 8.5 kcal mol^{-1} below (B3LYP*), 4.2 kcal mol^{-1} above (BP86), or 1.8 kcal mol^{-1} above (M06-L) the global minimum structure **Mn-1S** (Figs. 8 and S4, Table 4). This is another example of the tendency of the B3LYP* method to favor higher spin states relative to the BP86 method, as discussed by Reiher and collaborators [30, 31]. The Mn-C distances in **Mn-2T** indicate pentahapto coordination of each heptalene ring to a manganese atom. The predicted long Mn···Mn distance of 3.972 Å (B3LYP*), 4.001 Å (BP86), or 3.907 Å (M06-L) in **Mn-2T** confirms no direct bond between the two manganese atoms, thereby giving each manganese atom a 17-electron configuration for a binuclear triplet. However, the B3LYP* and M06-L methods for **Mn-2T** give significant spin contamination values, namely $\langle S^2 \rangle$ = 2.48 or 2.34, respectively.

$(C_{12}H_{10})_2Fe_2$

Five structures were optimized for $(C_{12}H_{10})_2Fe_2$ (Figs. 9 and S5, Table 5). The global minimum structure is the C_i singlet (η^4,η^6-$C_{12}H_{10})_2Fe_2$ structure **Fe-1S**, in which each iron atom is sandwiched between a hexahapto and a tetrahapto heptalene ring, as indicated by the Fe-C distances. The local iron environments in **Fe-1S** are similar to that in the known bis(cyclooctatetraene)iron [51], (η^4-C_8H_8)(η^6-

Table 5 Total energies (E in hartree), relative energies (ΔE in kcal mol^{-1}), HOMO-LUMO gaps (eV), Fe-Fe distances (Å), numbers of imaginary vibrational frequencies (Nimg), and spin expectation values $\langle S^2 \rangle$ for the $(C_{12}H_{10})_2Fe_2$ structures

	Fe-1S (C_i)			Fe-2S (D_{2h})		
	B3LYP*	BP86	M06-L	B3LYP*	BP86	M06-L
-HOMO(α)	0.14740	−0.12813	0.12625	0.13688	0.12755	0.12120
-LUMO(α)	0.05911	−0.08737	0.07337	0.07905	0.09910	0.09048
gap/eV	2.40	1.11	1.44	1.57	0.77	0.84
Fe-Fe	4.198	4.191	4.162	4.345	4.354	4.294
–E	3453.10193	−3454.50622	3453.88009	3453.08828	3454.49821	3453.86811
ΔE	0.0	0.0	0.0	8.6	5.0	7.5
Nimg	none	none	none	1(102i)	none	none
$\langle S^2 \rangle$	0.00	0.00	0.00	0.00	0.00	0.00
	Fe-3S (C_1)			Fe-4S (C_1)		Fe-5T (C_1)
	B3LYP*	BP86	M06-L	B3LYP*	M06-L	BP86
-HOMO(α)	0.15705	0.13759	0.13294	0.16524	0.14710	0.13062
-LUMO(α)	0.08157	0.10347	0.09275	0.08460	0.09953	0.09660
gap/eV	2.05	0.93	1.09	2.19	1.29	0.93
Fe-Fe	2.857	2.827	2.807	2.705	2.631	4.295
–E	3453.08493	3454.49596	3453.86434	3453.08609	3453.86418	3454.49450
ΔE	10.7	6.4	9.9	9.9	10.0	7.4
Nimg	none	none	none	none	none	none
$\langle S^2 \rangle$	0.00	0.00	0.00	0.00	0.00	2.17

$C_8H_8)_2Fe$. There is one uncomplexed C=C double bond in each heptalene ligand in **Fe-1S** with predicted lengths of 1.380 Å (B3LYP*), 1.395 Å (BP86), or 1.379 Å (M06-L). The long Fe···Fe distance of 4.198 Å (B3LYP*), 4.191 Å (BP86), or 4.162 Å (M06-L) in **Fe-1S** indicates no bond between the two iron atoms. Each iron atom in **Fe-1S** has the favored 18-electron configuration in this (η^4,η^6-$C_{12}H_{10})_2Fe_2$ structure with no iron-iron bond.

The second $(C_{12}H_{10})_2Fe_2$ structure is the more symmetrical D_{2h} singlet **Fe-2S**, lying 8.6 kcal mol^{-1} (B3LYP*), 5.0 kcal mol^{-1} (BP86), or 7.5 kcal mol^{-1} (M06-L) above the global minimum structure **Fe-1S** (Figs. 9 and S5, Table 5). Each iron atom in **Fe-2S** is sandwiched between two pentahapto heptalene rings. The predicted long Fe···Fe distance of 4.345 Å (B3LYP*), 4.354 Å (BP86), or 4.294 Å (M06-L) confirms the absence of a direct iron-iron bond in **Fe-2S,** so that the local iron environments are similar to that of the iron atom in ferrocene. However, an imaginary frequency of 102*i* cm^{-1} is predicted for **Fe-2S** by the B3LYP* method, although the BP86 method and M06-L method both predict all real.

The third $(C_{12}H_{10})_2Fe_2$ structure is the singlet C_1 structure **Fe-3S**, lying 10.7 kcal mol^{-1} (B3LYP*), 6.4 kcal mol^{-1} (BP86), or 9.9 kcal mol^{-1} (M06-L) above the global minimum structure **Fe-1S** (Figs. 9 and S5, Table 5). In **Fe-3S** each iron atom is coordinated to a tetrahapto subunit of one heptalene ligand and a pentahapto subunit of the other heptalene ligand. For one of the iron atoms the tetrahapto subunit has butadiene geometry whereas for the other iron the tetrahapto subunit has trimethylenemethane geometry. The predicted Fe-Fe distance of 2.857 Å (B3LYP*), 2.827 Å (BP86), or 2.807 Å (M06-L) is consistent with a formal single bond, thereby giving each iron atom the favored 18-electron configuration.

The fourth $(C_{12}H_{10})_2Fe_2$ structure **Fe-4S** is predicted by the B3LYP* and M06-L functionals (Figs. 9 and S5, Table 5). Using these two functionals, each iron atom is coordinated to two tetrahapto ligands, leaving two C=C double bonds of ~1.37 Å in each heptalene ligand. The calculated Fe=Fe distance of 2.705 Å (B3LYP*) or 2.631 Å (M06-L) can be interpreted as a formal double bond, thereby giving each iron atom the favored 18-electron configuration. Optimization by the BP86 functional starting with the **Fe-4S** geometry leads to **Fe-3S.**

The only triplet $(C_{12}H_{10})_2Fe_2$ structure **Fe-5T** was predicted by the BP86 method to lie 7.4 kcal mol^{-1} above the **Fe-1S** global minimum. The long Fe···Fe distance in **Fe-5T** of 4.295 Å clearly establishes the absence of direct iron-iron bonding. Attempted optimizations of **Fe-5T** using either the B3LYP* or M06-L methods failed owing to convergence problems.

$(C_{12}H_{10})_2Co_2$

Three $(C_{12}H_{10})_2Co_2$ structures were obtained for the binuclear cobalt compound (Figs. 10 and S6, Table 6). The C_1 singlet structure **Co-1S** is predicted by the BP86 method to be the global minimum. In **Co-1S**, one heptalene ligand (the "top" heptalene ligand in Fig. 10) uses the six carbon atoms of a hexatriene subunit to bond to the Co_2 system, leaving a hexatriene unit with three C=C uncomplexed double bonds of lengths 1.38±0.02 Å. The other heptalene ligand in **Co-1S** (the "bottom" heptalene ligand in Figs. 10 and S6) uses the eight carbon atoms of a heptafulvene subunit to bond to the Co_2 system, leaving an uncomplexed *cis*-1, 3-diene unit with two C=C uncomplexed double bonds of lengths ~1.38 Å. The Co–Co distance of 2.697 Å (B3LYP*), 2.649 Å (BP86), or 2.590 Å (M06-L) in **Co-1S** suggests a formal single bond, thereby giving one cobalt atom the preferred 18-electron configuration but the other cobalt atom only a 16-electron configuration.

The second $(C_{12}H_{10})_2Co_2$ structure is the C_1 singlet structure **Co-2S,** lying 7.7 kcal mol^{-1} (B3LYP*), 6.4 kcal mol^{-1} (BP86), or 7.3 kcal mol^{-1} (M06-L) above the global minimum structure **Co-1S** (Figs. 10 and S6, Table 6). The Co···Co distance of 4.019 Å (B3LYP*), 3.994 Å (BP86), or 3.951 Å (M06-L) in **Co-2S** suggests no direct cobalt-cobalt bond. In **Co-2S** one cobalt atom (Figs. 10

Table 6 Total energies (E in hartree), relative energies (ΔE in kcal mol^{-1}), HOMO-LUMO gaps (eV), Co-Co distances (Å), and spin expectation values $\langle S^2\rangle$ for the $(C_{12}H_{10})_2Co_2$ structures. None of these structures have any imaginary vibrational frequencies

	Co-1S (C_1)			Co-2S (C_1)			Co-3 T (C_s, C_{2v})		
	B3LYP*	BP86	M06-L	B3LYP*	BP86	M06-L	B3LYP*	BP86	M06-L
HOMO(α)	0.16163	0.13913	0.13985	0.15551	0.13521	0.13211	0.14561	0.12961	0.13330
LUMO(α)	0.09027	0.11311	0.10269	0.07899	0.10340	0.09320	0.07469	0.08471	0.08488
gap/eV	1.94	0.71	1.01	2.08	0.87	1.06	1.93	1.22	1.32
Co-Co	2.697	2.649	2.590	4.019	3.994	3.951	5.079	4.598	5.043
–E	3691.23677	3692.68057	3692.00451	3691.22443	3692.67038	3691.99280	3691.24003	3692.66810	3691.99930
ΔE	0.0	0.0	0.0	7.7	6.4	7.3	−2.1	7.8	3.3
$\langle S^2\rangle$	0.00	0.00	0.00	0.00	0.00	0.00	2.26	2.07	2.22

and S6) is sandwiched between a trihapto ring and a hexahapto ring, thereby attaining the favored 18-electron configuration. However, the other cobalt atom in **Co-2S** (Figs. 10 and S6) is sandwiched between a trihapto ring and a tetrahapto ring and thus has only a 16-electron configuration. This arrangement of bonding of the two heptalene rings to the cobalt atoms in **Co-2S** leaves an uncomplexed *cis*-diene unit and an isolated uncomplexed C=C double bond in one of the heptalene units (the "top" heptalene ligand in Fig. 10) and only an uncomplexed C=C double bond in the other heptalene unit (the "bottom" heptalene ligand in Figs. 10 and S6).

Different lowest energy triplet spin state structures **Co-3T** are predicted by three different methods for $(C_{12}H_{10})_2Co_2$ (Figs. 10 and S6, Table 6). For both structures the predicted Co···Co distances greater than 4.5 Å preclude any possibility of direct cobalt-cobalt bonding. The B3LYP* method and M06-L method predict a C_s structure for **Co-3T** with one cobalt atom sandwiched between two tetrahapto heptalene rings and the other cobalt atom sandwiched between two trihapto heptalene rings. This provides one cobalt atom with a 17-electron configuration but the other cobalt atom with only a 15-electron configuration. This is nevertheless consistent with a binuclear triplet. The BP86 method predicts a more symmetrical C_{2v} structure for **Co-3T** in which each cobalt atom is sandwiched between two tetrahapto heptalene rings thereby giving each cobalt atom a 17-electron configuration for a binuclear triplet. The B3LYP* method predicts **Co-3T** to lie 2.1 kcal mol^{-1} below **Co-1S** whereas the BP86 method and M06-L method predict **Co-3T** to lie 7.8 kcal mol^{-1} or 3.3 kcal mol^{-1} above **Co-1S,** respectively. However, a relatively large spin contamination value of $\langle S^2 \rangle = 2.26$ or 2.22, respectively (versus an ideal value of 2.0 for a triplet) was obtained by the B3LYP* method or the M06-L method for the triplet **Co-3T**. This suggests that the B3LYP* and M06-L structure optimizations for **Co-3T** might be less reliable than the BP86 optimization with $\langle S^2 \rangle = 2.07$.

$(C_{12}H_{10})_2Ni_2$

Four $(C_{12}H_{10})_2Ni_2$ structures were optimized, namely **Ni-1S, Ni-2S, Ni-3S**, and **Ni-4T** (Figs. 11 and S7, Table 7). The global minimum structure is the C_s singlet **Ni-1S.** The Ni-C distances in **Ni-1S** indicate that each heptalene ring functions as a trihapto ligand, so that each nickel atom is sandwiched between two trihapto heptalene rings. The predicted Ni···Ni distance of 5.188 Å (B3LYP*), 5.128 Å (BP86), or 5.127 Å (M06-L) in **Ni-1S** clearly indicates the absence of direct bonding between the nickel atoms. Therefore, each nickel atom in **Ni-1S** attains the 16-electron configuration.

The second predicted $(C_{12}H_{10})_2Ni_2$ structure is the C_1 singlet **Ni-2S**, lying only 4.2 kcal mol^{-1} (B3LYP*), 0.6 kcal mol^{-1} (BP86), or 2.7 kcal mol^{-1} (M06-L) in energy above **Ni-1S** (Figs. 11 and S7, Table 7). The Ni-C distances in **Ni-2S** suggest that each heptalene ring of the "top" heptalene functions as a trihapto ligand, while each heptalene ring of the "bottom" heptalene functions as a tetrahapto ligand. This leaves an uncomplexed *cis*-1,3-diene unit and an

Table 7 Total energies (E in hartree), relative energies (ΔE in kcal mol^{-1}), HOMO-LUMO gaps (eV), Ni-Ni distances (Å), numbers of imaginary vibrational frequencies, and spin expectation values $\langle S^2 \rangle$ for the $(C_{12}H_{10})_2Ni_2$ structures

	B3LYP*	BP86	M06-L	B3LYP*	BP86	M06-L
	Ni-1S (C_s)			Ni-2S (C_1)		
HOMO(α)	0.14991	0.13992	0.12754	0.15531	0.14633	0.14312
LUMO(α)	0.07558	0.09573	0.08578	0.08367	0.10174	0.09310
gap/eV	2.02	1.20	1.14	1.95	1.21	1.36
Ni-Ni	5.188	5.128	5.127	2.805	2.748	2.658
–E	3942.36764	3943.82559	3943.11911	3942.36095	3943.82459	3943.11484
ΔE	0.0	0.0	0.0	4.2	0.6	2.7
Nimg	none	none	none	none	none	none
$\langle S^2 \rangle$	0.00	0.00	0.00	0.00	0.00	0.00
	Ni-3S (C_{2v})			Ni-4T (C_1)		
HOMO(α)	0.13577	0.13101	0.12754	0.13198	0.11777	0.11510
LUMO(α)	0.08062	0.09641	0.08578	0.07497	0.09060	0.08234
gap/eV	1.50	0.94	1.09	1.55	0.74	0.89
Ni-Ni	4.701	4.753	4.820	5.158	5.114	5.072
–E	3942.35793	3943.82183	3943.11268	3942.34293	3943.79765	3943.09270
ΔE	6.1	2.4	4.0	15.5	17.5	16.6
Nimg	none	none	2(90i,32i)	none	none	none
$\langle S^2 \rangle$	0.00	0.00	0.00	2.06	2.01	2.04

isolated uncomplexed C=C double bond in the "top" heptalene ligand. In the "bottom" heptalene ligand the eight carbons bonded to the Ni_2 unit form a heptafulvene subunitt leaving an uncomplexed *cis*-1,3-diene unit. The five uncomplexed C=C double bonds in structure **Ni-2S** are relatively short at 1.38±0.02 Å. The predicted Ni-Ni distance of 2.805 Å (B3LYP*), 2.748 Å (BP86), or 2.658 Å (M06-L) in **Ni-2S** can be interpreted as a formal single bond leading to the favored 18-electron configuration for each nickel atom. The Ni–Ni distance predicted for **Ni-2S** is ~0.1 Å longer than the Ni-Ni distance of 2.730 Å (B3LYP) or 2.672 Å (BP86) predicted for $Ni_2(CO)_6(\mu\text{-}CO)$ in a previous DFT study [52].

The third $(C_{12}H_{10})_2Ni_2$ structure is a C_{2v} singlet structure **Ni-3S**, lying only 6.1 kcal mol^{-1} (B3LYP*), 2.4 kcal mol^{-1} (BP86), or 4.0 kcal mol^{-1} (M06-L) in energy above **Ni-1S** (Figs. 11 and S7, Table 7). The Ni-C distances in **Ni-3S** indicate that each heptalene ring functions as a tetrahapto ligand, so that each nickel atom is sandwiched between two tetrahapto heptalene rings. The predicted Ni···Ni distance of 4.701 Å (B3LYP*), 4.753 Å (BP86), or 4.820 Å (M06-L) in **Ni-3S** indicates the absence of direct bonding between the nickel atoms. Therefore, each nickel atom in **Ni-3S** attains the favored 18-electron configuration. Two imaginary vibrational frequencies of 90*i* and 32*i* cm^{-1} were predicted by the M06-L method. However, the B3LYP* and BP86 methods predicted all real ones. Following the normal mode of the largest imaginary frequency it goes to **Ni-1S.**

A triplet $(C_{12}H_{10})_2Ni_2$ structure is also found, namely **Ni-4T** lying 15.5 kcal mol^{-1} (B3LYP*), 17.5 kcal mol^{-1} (BP86), or 16.6 kcal mol^{-1} (M06-L) above **Ni-1S** (Figs. 11 and S7, Table 7). The Ni-C distances indicate that one of the two nickel atoms (Figs. 11 and S7) is sandwiched between a trihapto and a tetrahapto heptalene ring whereas the other nickel atom (Figs. 11 and S7) is sandwiched between a dihapto and a pentahapto heptalene ring. The very long Ni···Ni distance of 5.158 Å (B3LYP*), 5.114 Å (BP86), or 5.072 Å (M06-L) in **Ni-4T** indicates the absence of a direct nickel-nickel bond, thereby giving each nickel atom the 17-electron configuration for a binuclear triplet.

Discussion

The global minimum structure predicted for $(C_{12}H_{10})_2Ti_2$ is the triplet $(\eta^5,\eta^7\text{-}C_{12}H_{10})_2Ti_2$ structure **Ti-1T** (Fig. 5). The predicted Ti-Ti distance of 3.371 Å (B3LYP*), 3.478 Å (BP86), or 3.310 Å (M06-L) can be interpreted as a formal single bond thereby giving each Ti atom the 17-electron configuration. The lowest energy structures for the other two first row early transition metal binuclear compounds display the $(\eta^7,\eta^7\text{-}C_{12}H_{10})_2M_2$ (M = V, Cr) bonding motifs, in which all of the 12 carbon atoms of each heptalene ligand lie within bonding distance of a metal atom. The metal-metal distances in these structures of 3.4 Å or greater dictate the absence of a direct metal-metal bond. Dividing the 12 π electrons of each heptalene ligand equally between the metal atoms gives the metal atoms 17- and 18-electron configurations for the vanadium and chromium derivatives, respectively, similar to the metal environments in the known mononuclear derivatives $(\eta^6\text{-}C_6H_6)_2M$ (M = Ti, V, Cr) and $(\eta^5\text{-}C_5H_5)(\eta^7\text{-}C_7H_7)M$ (M = Ti, V, Cr), respectively. For $(C_{12}H_{10})_2Ti_2$ the three stable structures **Ti-1T, Ti-2S**, and **Ti-3S** are essentially degenerate predicted by the BP86 method. For $(\eta^7,\eta^7\text{-}C_{12}H_{10})_2V_2$ the triplet state, which has an unpaired electron on each vanadium atom corresponding to their 17-electron configurations, lies significantly in energy below the singlet state **V-2S**. In singlet **V-2S** the V-V distance of ~3.5 Å can be interpreted as the formal single bond required to give both vanadium atoms the favored 18-electron configuration. However, this V-V bond appears to be rather long, apparently because of the constraints of the heptahapto bonding of the vanadium atoms to each heptalene ring.

The chromium system $(C_{12}H_{10})_2Cr_2$ is interesting since two structures are very closely spaced in energy. Thus, both a singlet structure **Cr-1S** and a triplet structure **Cr-2T** are found. In **Cr-2T** one of the chromium atoms is sandwiched between a heptahapto heptalene ring and a pentahapto heptalene ring and thus has a local environment similar to the known [48, 49] diamagnetic $(\eta^5\text{-}C_5H_5)(\eta^7\text{-}C_7H_7)Cr$ with an 18-electron configuration. However, the other chromium atom in **Cr-2T** is sandwiched between two pentahapto heptalene rings and thus has a local environment similar to the known [47] 16-electron triplet state $(\eta^5\text{-}C_5H_5)_2Cr$.

The other type of structure found for the early transition metal derivatives $(C_{12}H_{10})_2M_2$ (M = V, Cr, Mn) has one approximately planar heptalene ligand bonded to the central M_2 unit through all 12 carbon atoms. The other heptalene ligand is highly non-planar and uses only eight carbon atoms of a heptafulvene subunit for bonding to the central M_2 unit, leaving an uncomplexed *cis*-1,3-diene unit

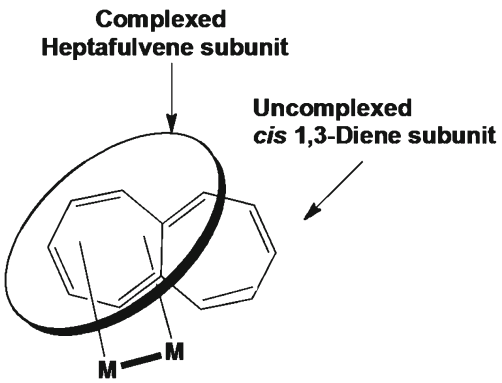

Fig. 12 Partition of the heptalene ligand into a complexed heptafulvene subunit and an uncomplexed *cis*-1,3-diene subunit as found in the $(C_{12}H_{10})_2M_2$ structures V-3S, Cr-3S, and Mn-1S

(Fig. 12). This heptafulvene bonding mode of the non-planar heptalene ligand brings the metals of the central M_2 unit close enough for a direct metal-metal bond. These metal-metal distances suggest formal single, double, and triple bonds for the manganese derivative **Mn-1S** (Fig. 8), the chromium derivative **Cr-3S** (Fig. 7), and vanadium derivative **V-3S** (Fig. 6), respectively. This gives the metal atoms the favored 18-electron configurations in all three of these structures. For the analogous titanium derivative **Ti-3S** (Fig. 5), the titanium-titanium distance of ~2.70 Å is clearly longer than the V≡V distance of ~2.50 Å, so assignment of a formal bond order of four for the Ti-Ti bond in **Ti-3S** is clearly unreasonable. The predicted ~2.70 Å Ti≡Ti distance in **Ti-3S** is close to the Ti≡Ti distance of ~2.80 Å predicted [40] for the Ti≡Ti triple bond in $(\eta^5\text{-}C_5H_5)_2Ti_2(CO)_6$, suggesting a formal triple bond in **Ti-3S**. This gives one titanium atom in **Ti-3S** the favored 18-electron configuration but the other titanium atom only a 16-electron configuration.

The iron complex $(C_{12}H_{10})_2Fe_2$ might be expected to exhibit a singlet structure in which each iron atom is sandwiched between two pentahapto heptalene rings with local environments similar to that in the very stable ferrocene $(\eta^5\text{-}C_5H_5)_2Fe$ with the favored 18-electron configuration. A singlet D_{2h} structure of this type, namely **Fe-2S** (Fig. 9), is found, with a geometry very similar to that of the triplet $(C_{12}H_{10})_2Mn_2$ structure **Mn-2T**. However, the lowest energy $(C_{12}H_{10})_2Fe_2$ structure **Fe-1S** has non-planar heptalene ligands with each iron atom sandwiched between a hexahapto heptalene ring and a tetrahapto heptalene ring. The local iron environments in **Fe-1S** are thus similar to that in the known bis(cyclooctatetraene)iron [51], $(\eta^4\text{-}C_8H_8)(\eta^6\text{-}C_8H_8)_2Fe$.

The late transition metals cobalt and nickel require fewer electrons to approach the favored 18-electron configuration so the heptalene rings are only partially bonded to the metal atoms in the $(C_{12}H_{10})_2M_2$ (M=Co, Ni) structures. The cobalt system $(C_{12}H_{10})_2Co_2$ is the most complicated of the $(C_{12}H_{10})_2M_2$ systems with challenging differentiations between bonding and non-bonding metal-carbon distances. The metal-ring bonding in the unsymmetrical singlet $(C_{12}H_{10})_2Co_2$ structure **Co-1S** with non-planar heptalene ligands can best be interpreted with one cobalt atom sandwiched between hexahapto and trihapto heptalene rings and the other cobalt atom sandwiched between tetrahapto and trihapto heptalene rings. This gives the first cobalt atom the favored 18-electron configuration but the second cobalt atom only a 16-electron configuration. Such 16-electron configurations are not unusual in late transition metal complexes in which assignment of formal oxidation states can have the metal in a d^8 configuration.

In the lowest energy singlet structure **Ni-1S** the nickel atoms are too far apart (~5.1 Å) for a direct metal-metal bond. Each nickel atom is sandwiched between two trihapto heptalene rings to attain only a 16-electron configuration. The slightly higher energy $(C_{12}H_{10})_2Ni_2$ structure **Ni-2S** has six carbons of one heptalene unit and eight carbons of the other heptalene unit bonded to the pair of nickel atoms (Fig. 11). A Ni-Ni single bond of length ~2.74 Å then provides each metal atom with the favored 18-electron configuration. Another slightly higher energy structure **Ni-3S** has each nickel atom sandwiched between two tetrahapto heptalene rings to attain the favored 18-electron configuration. The higher energy triplet $(C_{12}H_{10})_2Ni_2$ structure **Ni-4T** has each nickel atom sandwiched between seven heptalene carbon atoms. Thus one nickel atom is sandwiched between a trihapto and a tetrahapto heptalene ring and the other nickel atom is sandwiched between a dihapto and a pentahapto heptalene ring. This gives each nickel atom the 17-electron configuration corresponding to a binuclear triplet.

Conclusions

The bis(heptalene)dimetal complexes $(C_{12}H_{10})_2M_2$ of the first row transition metals from Ti to Ni are predicted by density functional theory to have a "submarine" sandwich structure with a pair of metal atoms sandwiched between the two heptalene rings. For the early transition metal derivatives $(C_{12}H_{10})_2M_2$ (M = V, Cr) there are two types of structures. In one structural type the metals are sandwiched between two heptahapto heptalene rings with metal-metal distances (3.5–3.8 Å) too long for direct metal-metal bonding. Partitioning the 12 π-electrons of the heptalene rings equally between the two metals gives the central vanadium and chromium atoms 17- and 18-electron configurations corresponding to triplet and singlet spin states, respectively. The other type of $(C_{12}H_{10})_2M_2$ (M = V, Cr, Mn) structure has a pair of bonded metal atoms sandwiched between a fully bonded heptalene ligand and a heptalene ligand bonded to the metals only through an eight-carbon heptafulvene subunit, leaving an uncomplexed *cis*-1,3-diene unit. The formal metal-metal bond orders in these latter structures are 3, 2, and 1 for M = V, Cr, and Mn with predicted bond lengths of 2.5, 2.7, and 2.8 Å, respectively.

The titanium system $(C_{12}H_{10})_2Ti_2$ is unusual since three different structural types have essentially the same energies. These include singlet and triplet state structures with each titanium atom sandwiched between two heptahapto heptalene rings as well as a singlet structure in which the Ti_2 unit is sandwiched between a fully bonded heptalene ligand and a second partially bonded heptalene ligand.

Different types of structures are predicted for the later transition metal derivatives $(C_{12}H_{10})_2M_2$ (M=Fe, Co, Ni), which require fewer electrons from the heptalene unit to attain the favored 18-electron configuration. For the iron derivative $(C_{12}H_{10})_2Fe_2$ a singlet structure with each iron

atom sandwiched between a hexahapto and a tetrahapto heptalene ring is energetically preferred over an alternate structure with ferrocene-like iron atoms sandwiched between two pentahapto heptalene rings. Partial bonding of each heptalene ring to the metal atoms occurs in the late transition metal derivatives $(C_{12}H_{10})_2M_2$ (M=Co, Ni). This leads to an unsymmetrical structure for the cobalt derivative and a structure for the nickel derivative with each nickel atom sandwiched between a trihapto ligand and a tetrahapto ligand.

Acknowledgments The research was supported by the Scientific Research Fund of the Key Laboratory of the Education Department of Sichuan Province (Grant No. 10ZX012), the fund of the Key Laboratory of Advanced Scientific Computation, Xihua University, the Program for New Century Excellent Talents in University (Grant No. NCET-10-0949), China, and the U. S. National Science Foundation (CHE-1057466 and CHE-1054286) for the support of this research.

References

1. Kealy TJ, Pauson PL (1961) Nature 168:1039–1040
2. Miller SA, Tebboth JA, Tremaine JF (1952) J Chem Soc 1952:632–635
3. Fischer EO, Hafner W (1955) Z Naturforsch 10(12):665–668
4. Elschenbroich C, Moeckel R, Massa W, Birkhahn M, Zenneck U (1982) Chem Ber 115(1):334–345
5. Katz TJ, Acton N, McGinnis J (1972) J Am Chem Soc 94 (17):6205–6206
6. Katz TJ, Acton N (1972) J Am Chem Soc 94(9):3281–3283
7. Ashley AE, Cooper RT, Wildgoose GG, Green JC, O'Hare D (2008) J Am Chem Soc 130(46):15662–15667
8. Cloke FGN, Green JC, Jardine CN, Kuchta MC (1999) Organometallics 18(6):1087–1090
9. Balazs G, Cloke FGN, Gagliardi L, Green JC, Harrison A, Hitchcock PB, Shahi ARM, Summerscales OT (2008) Organometallics 27(9):2013–2020
10. Balazs G, Cloke FGN, Harrison A, Hitchcock PB, Green JC, Summerscales OT (2007) Chem Commun 2007:873–875
11. Dauben HJD, Bertelli DJ (1961) J Am Chem Soc 83(22):4659–4660
12. Vogel E, Königshofen H, Wassen J, Müllen K, Oth JFM (1974) Angew Chem Int Ed Engl 13(11):732–734
13. Vogel E, Königshofen H, Wassen J, Müllen K, Oth JFM (1974) Angew Chem 86(21):777–778
14. Vogel E, Kerimis D, Allison NT, Zellerhoff R, Wassen J (1979) Angew Chem Int Ed Engl 18(7):545–546
15. Müllen K, Allison NT, Lex J, Schmickler H, Vogel E (1987) Tetrahedron 43(14):3225–3236
16. Grimm FW, Hafner K, Lindner HJ (1996) Chem Ber 129 (12):1569–1572
17. Dunning TH (1970) J Chem Phys 53(7):2823–2833
18. Huzinaga S (1965) J Chem Phys 42(4):1293–1302
19. Wachters AJ H (1970) J Chem Phys 52(2):1033–1036
20. Hood DM, Pitzer RM, Schaefer HF (1979) J Chem Phys 71 (2):705–712
21. Ziegler T, Autschbach J (2005) Chem Rev 105(6):2695–2722
22. Bühl M, Kabrede H (2006) J Chem Theory Comput 2(5):1282–1290
23. Brynda M, Gagliardi L, Widmark PO, Power PP, Roos BO (2006) Angew Chem Int Ed 45(23):3804–3807
24. Sieffert N, Bühl M (2010) J Am Chem Soc 132(23):8056–8070
25. Schyman P, Lai W, Chen H, Wang Y, Shaik S (2011) J Am Chem Soc 133(2):7977–7984
26. Adams RD, Pearl WC, Wong YO, Zhang Q, Hall MB, Walensky JR (2011) J Am Chem Soc 133(33):12994–12997
27. Lonsdale R, Olah J, Mulholland AJ, Harvey JA (2011) J Am Chem Soc 133(35):15464–15474
28. Becke AD (1993) J Chem Phys 98(7):5648–5652
29. Lee C, Yang W, Parr RG (1988) Phys Rev B 37(2):785–789
30. Reiher M, Salomon O, Hess BA (2001) Theor Chem Acc 107:48–55
31. Salomon O, Reiher M, Hess BA (2002) J Chem Phys 117 (10):4729–4737
32. Stokes FA, Less RJ, Haywood J, Melen RL, Thompson RI, Wheatley AEH, Wright DS (2012) Organometallics 31(1):23–26
33. Becke AD (1988) Phys Rev A 38(6):3098–3100
34. Perdew JP (1986) Phys Rev B 33(12):8822–8824
35. Zhao Y, Truhlar DG (2008) Theor Chem Acc 120:215–241
36. Frisch MJ et al. (2009) Gaussian 09, revision A.02. Gaussian Inc, Wallingford
37. Papas BN, Schaefer HF (2006) J Mol Struct (THEOCHEM) 768 (1–3):175–181
38. Zeinstra JD, De Boer JL (1973) J Organomet Chem 54:207–211
39. Tairova GG, Krasochka ON, Ponomarev VI, Kvashina EF, Shvetsov YA, Lisetskii EM, Kiryukhin DP, Atovmyan LO, Borodko YG (1982) Transit Met Chem 7:189–190
40. Zhang X, Li QS, Xie Y, King RB, Schaefer HF (2010) Inorg Chem 49(4):1961–1975
41. King RB, Stone FGA (1959) J Am Chem Soc 81(19):5263–5264
42. Engebretson G, Rundle RE (1963) J Am Chem Soc 85(4):481–482
43. Fischer EO, Kogler HP (1957) Chem Ber 90(2):250–255
44. Zhang X, Li Q, Xie Y, King RB, Schaefer HF (2007) Eur J Inorg Chem 11:1599–1605
45. Cotton FA, Kruczynski L (1978) J Organomet Chem 160(1):93–100
46. Huffman JC, Lewis LN, Caulton KG (1980) Inorg Chem 19 (9):2755–2762
47. Weiss E, Fischer EO (1956) Z Anorg Allg Chem 284(103):69–72
48. King RB, Bisnette MB (1964) Inorg Chem 3(6):785–790
49. Braunschweig H, Kupfer T, Lutz M, Radacki K (2007) J Am Chem Soc 129(28):8893–8906
50. Martin M, Rees B, Mitschler A (1982) Acta Crystallogr B 38:6–15
51. Allegra G, Colombo A, Immirzi A, Bassi IW (1968) J Am Chem Soc 90(16):4455–4456
52. Ignatyev IS, Schaefer HF, King RB, Brown ST (2000) J Am Chem Soc 122(9):1989–1994